Loosely bound states of three particles

Zheng Zhen and Joseph Macek
Department of Physics and Astronomy, University of Nebraska–Lincoln, Lincoln, Nebraska 68588
(Received 3 March 1988)

The adiabatic hyperspherical technique is applied to a three-body system interacting via a short-range potential. Analytical expressions for the effective hyper-radial potential have been obtained without explicit use of the two-body potential. Possible loosely bound states of the system have been analyzed quantitatively and the result confirms the prediction by V. Efimov (Yad. Fiz. **10**, 107 (1969) [Sov. J. Nucl. Phys. **10**, 62 (1970)]). At the same time, some new characteristics of the three-body system are obtained.

I. INTRODUCTION

The three-body problem has long been investigated from widely different perspectives.[1–7] Up to now, however, most atomic and molecular problems are still studied using the well-established principles for two-body systems or their extensions. Although the success of the new conventional multiple-scattering expansion[1,2] is recognized, such methods have not revealed some important physical properties of many-body systems. This was made clear by Efimov[7] in 1970 when he found theoretically that loosely bound states exist for systems of three bosons interacting via short-range two-body potentials. The number of bound states which Efimov predicted is given by

$$N=\frac{1}{\pi}\ln\frac{|c_0|}{r_0}\ , \tag{1}$$

where c_0 and r_0 are, respectively, the scattering length and the effective range for the assumed two-body potential.[8] As c_0 goes to infinity, an infinite number of loosely bound states with an exponential condensation towards zero suddenly appear. But for a finite c_0, the number of bound states decrease sharply because of the logarithmic relation between N and c_0, with the result that only one or two bound states can be observed in general. This mathematical model has been used to analyze the structure of clusters such as $^{12}C_3$, helium trimers, etc. Several groups[9] have studied the Efimov states in such systems numerically and the number of bound states they find is approximately the same as that given by Eq. (1) as long as N is rounded up to an appropriate integer. Although there is no corresponding experimental data to confirm these results at present, the theory is nevertheless of great interest because it predicts some new physical properties of three-body systems, among which the most remarkable one is the existence of loosely bound states in such systems, even though the interaction potential between the particles has no wells strong enough to bind any two of the three particles separately. Because of this, and since the three-body system is the simplest model in many-body problems, it seems desirable to use the three-body system (instead of two-body) as the basic block of the many-body system. This requires more extensive study of the three-body system.

In a previous paper,[10] Macek developed the theory of Efimov by applying the adiabatic-hyperspherical-coordinate approximation to study the dynamics of three neutral atoms interacting with each other on a general potential surface. Under this approximation, Efimov's result for finite scattering length can be reproduced by the variational method. The effective potential in hyperspherical coordinates thus obtained is exactly the same as Efimov's, namely,

$$U_\mu(R)=-\frac{4+t^2}{2mR^2}\ \text{ as } R\to\infty \tag{2}$$

with the variational constant $t=1.00624$. Evidently, such a potential will support an infinite number of bound states condensing to zero energy.[7]

Equation (2) holds only when the two-body scattering length is infinite. This paper considers the more general situation where the scattering length is finite but greater than the range of the two-body forces. We seek the potential $U_\mu(R)$ in this case. Using this potential we then solve the hyper-radius equation in the outer region for $R>r_0$ and obtain the logarithmic derivative $B(E)$ on a surface $R=R_0$. Knowledge of $B(E)$ versus E then enables one to estimate the number of bound states by using the standard assumptions of Wigner's R-matrix theory. It is also possible to estimate the energies of the bound states.

In Sec. II, we introduce some mathematical approaches which are frequently used when dealing with three-body systems and briefly review the adiabatic-hyperspherical-coordinate approximation. Section III is devoted to the analytical calculation of the potential curve, while the numerical analysis of the possible loosely bound states is given in Sec. IV. In Sec. V, we discuss the results obtained.

II. METHOD

A. Jacobi coordinates and the kinematic rotation

For a system of three particles with mass $m_i (i=1,2,3)$ as shown in Fig. 1, the Jacobi coordinates have been

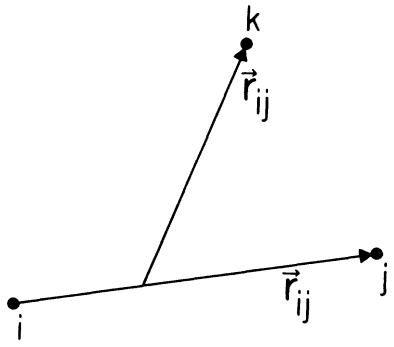

FIG. 1. Definition of Jacobi coordinates.

shown to be suitable to describe its physical behavior.[11] Generally, they are defined in Fig. 1 as

$$\mathbf{r}_{ij}=\mathbf{r}_j-\mathbf{r}_i \ , \tag{3}$$

$$\mathbf{r}_{ij,k}=\mathbf{r}_k-\frac{m_i\mathbf{r}_i+m_j\mathbf{r}_j}{m_i+m_j} \ , \tag{4}$$

where (i,j,k) form a cyclic permutation. Obviously, $\mathbf{r}_{ij}$ is the displacement vector of the particle j relative to i, and $\mathbf{r}_{ij,k}$ is the coordinate of the particle k relative to the center of mass of the other two particles. Corresponding to these coordinates we have two different reduced masses

$$m_{ij}=\frac{m_i m_j}{m_i+m_j} \ , \tag{5}$$

$$m_{ij,k}=\frac{(m_i+m_j)m_k}{m_i+m_j+m_k} \ . \tag{6}$$

Since

$$m_{ij}m_{ij,k}=\frac{m_i m_j m_k}{m_i+m_j+m_k} \ , \tag{7}$$

the product of m_{ij} and $m_{ij,k}$ is independent of the permutation of i, j, and k. This property is useful in simplifying the formula expressed in Jacobi coordinates.

By permuting the subscripts i, j, and k, we can get different sets of Jacobi coordinates. But, since

$$\mathbf{r}_{ij}=-\mathbf{r}_{ji} \ ,$$

$$\mathbf{r}_{ij,k}=\mathbf{r}_{ji,k} \ ,$$

we need only three independent sets of Jacobi coordinates. For definiteness we choose them as $(\mathbf{r}_{ij},\mathbf{r}_{ij,k})$, where (i,j,k) form an even permutation of (1,2,3). From Fig. 1, it is obvious that the alternative sets are connected by the so-called kinematic rotation[12]

$$\sqrt{m_{ki}}\,\mathbf{r}_{ki}=-\cos\gamma(\sqrt{m_{ij}}\,\mathbf{r}_{ij})-\sin\gamma(\sqrt{m_{ij,k}}\,\mathbf{r}_{ij,k}) \ , \tag{8}$$

$$\sqrt{m_{ki,j}}\,\mathbf{r}_{ki,j}=\sin\gamma(\sqrt{m_{ij}}\,\mathbf{r}_{ij})-\cos\gamma(\sqrt{m_{ij,k}}\,\mathbf{r}_{ij,k}) \ , \tag{9}$$

with

$$\tan\gamma=\frac{m_i}{\sqrt{m_{ij}m_{ij,k}}} \ , \tag{10}$$

and

$$\sqrt{m_{jk}}\,\mathbf{r}_{jk}=-\cos\gamma'(\sqrt{m_{ij}}\,\mathbf{r}_{ij})+\sin\gamma'(\sqrt{m_{ij,k}}\,\mathbf{r}_{ij,k}) \ , \tag{11}$$

$$\sqrt{m_{jk,i}}\,\mathbf{r}_{jk,i}=-\sin\gamma'(\sqrt{m_{ij}}\,\mathbf{r}_{ij})-\cos\gamma'(\sqrt{m_{ij,k}}\,\mathbf{r}_{ij,k}) \ , \tag{12}$$

with

$$\tan\gamma'=\frac{m_j}{\sqrt{m_{ij}m_{ij,k}}} \ . \tag{13}$$

For the particular case of three identical particles with mass m_0 we have

$$m_{ij}=\tfrac{1}{2}m_0 \ , \tag{14}$$

$$m_{ij,k}=\tfrac{2}{3}m_0 \ , \tag{15}$$

$$\gamma=\gamma'=\frac{\pi}{3} \ . \tag{16}$$

Now, in terms of Jacobi coordinates, the kinetic energy operator in the center-of-mass system can be expressed as

$$H_0=\frac{\mathbf{P}_{ij}^2}{2m_{ij}}+\frac{\mathbf{P}_{ij,k}^2}{2m_{ij,k}} \ , \tag{17}$$

where $\mathbf{P}_{ij}$ and $\mathbf{P}_{ij,k}$ are, respectively, the conjugate momenta of $\mathbf{r}_{ij}$ and $\mathbf{r}_{ij,k}$. The physical interpretation of Eq. (17) is straightforward. The first term corresponds to the relative kinetic energy of particles i and j in their own center-of-mass system and the second term accounts for the relative kinetic energy of particle k with the compound system i and j.

B. Adiabatic hyperspherical approximation

Suppose that the interaction between the particles is via some kind of two-body potential. Then, in terms of Jacobi coordinates, the nonrelativistic, time-independent Schrödinger equation for the system considered with the motion of center of mass separated out is given by

$$\left[-\frac{1}{2m_{ij}}\nabla^2_{\mathbf{r}_{ij}}-\frac{1}{2m_{ij,k}}\nabla^2_{\mathbf{r}_{ij,k}}+V(\mathbf{r}_{ij},\mathbf{r}_{ij,k})\right]\Psi=E\Psi \ , \tag{18}$$

where E is the energy of the three-body cluster in the center-of-mass coordinate system.

For each set of Jacobi coordinates $(\mathbf{r}_{ij},\mathbf{r}_{ij,k})$, we introduce a new set of hyperspherical coordinates R, α_{ij}, r_{ij}, and $r_{ij,k}$, where R and α_{ij} are defined in terms of r_{ij} and $r_{ij,k}$ as[13]

$$mR^2=m_{ij}r_{ij}^2+m_{ij,k}r_{ij,k}^2 \ , \tag{19}$$

$$\tan\alpha_{ij}=\left[\frac{m_{ij}}{m_{ij,k}}\right]^{1/2}\frac{r_{ij}}{r_{ij,k}} \ . \tag{20}$$

Here the constant m with the dimension of mass is introduced so that R has the dimension of distance. Evidently, MR^2 should not depend on the permutation of the

subscripts i, j, and k, since the transformations given by Eqs. (8)–(13) are orthogonal. This allows us to switch to any set of Jacobi coordinates freely.

Generally speaking, the choice of m is arbitrary. But from Eq. (19) we can see that in order that the hyperspherical radius R has some more intuitive geometrical and physical meaning, it is useful to choose m equal to the mass of the particle. Only this kind of choice makes R measured in the same scale as that in which we measure r_{ij} and $r_{ij,k}$. We will come back to this point later.

The kinematic rotation of Eqs. (8)–(10) can now be expressed in the new coordinates as

$$\sin\alpha_{ki}\hat{\mathbf{r}}_{ki}=-\cos\gamma\sin\alpha_{ij}\hat{\mathbf{r}}_{ij}-\sin\gamma\cos\alpha_{ij}\hat{\mathbf{r}}_{ij,k}\ , \tag{21}$$

$$\cos\alpha_{ki}\hat{\mathbf{r}}_{ki,j}=\sin\gamma\sin\alpha_{ij}\hat{\mathbf{r}}_{ij}-\cos\gamma\cos\alpha_{ij}\hat{\mathbf{r}}_{ij,k}\ , \tag{22}$$

and the other one, of Eqs. (11)–(13), can be written down in the same way. Obviously, we have

$$\alpha_{ki}(\alpha_{ij}=0)=\gamma\ . \tag{23}$$

Now, in hyperspherical coordinates, Eq. (18) becomes

$$\left[-\frac{1}{2m}\left[\frac{d^2}{dR^2}+\frac{5}{R}\frac{d}{dR}-\frac{\Lambda^2}{R^2}\right]+V(R,\Omega)\right]\Psi=E\Psi\ , \tag{24}$$

where the generalized angular momentum operator Λ^2 is given by

$$\Lambda^2=-\left[\frac{d^2}{d\alpha_{ij}^2}+4\cot(2\alpha_{ij})\frac{d}{d_{ij}}\right]+\frac{l_{ij}^2}{\sin^2\alpha_{ij}}+\frac{l_{ij,k}^2}{\cos^2\alpha_{ij}}\ , \tag{25}$$

and l_{ij} and $l_{ij,k}$ are conventional angular momentum operators related to $\hat{\mathbf{r}}_{ij}$ and $\hat{\mathbf{r}}_{ij,k}$, respectively.

By the adiabatic hyperspherical approximation, we keep only the diagonal-coupling term and write

$$\Psi=\sum_{\mu}F_{\mu}(R)\Phi_{\mu}(R,\Omega)\cong F_{\mu}(R)\Phi_{\mu}(R,\Omega)\ . \tag{26}$$

Then Eq. (24) is parametrically separated into the radial equation

$$\left[-\frac{1}{2m}\left[\frac{d^2}{dR^2}+\frac{5}{R}\frac{d}{dR}\right]+U_{\mu}(R)+W_{\mu\mu}(R)\right]F_{\mu}(R)=EF_{\mu}(R) \tag{27}$$

and the angular one

$$U(R)\Phi_{\mu}(R,\Omega)=U_{\mu}(R)\Phi_{\mu}(R,\Omega)\ , \tag{28}$$

with

$$W_{\mu\mu}(R)=\left[\Phi_{\mu},\frac{d^2}{dR^2}\Phi_{\mu}\right]+2\left[\Phi_{\mu},\frac{d}{dR}\Phi_{\mu}\right]\frac{d}{dR} \tag{29}$$

and

$$U(R)=\frac{\Lambda^2}{2mR^2}+V(R,\Omega)\ . \tag{30}$$

We have seen that our problem has been approximated divided into two parts. The first one is solving the angular equation to obtain the channel potential; the second one is solving the one-dimensional radial equation to find the bound states. Once the channel potential $U_{\mu}(R)$ is determined, the original many-body problem reduces to a one-body problem, namely, finding the bound states of a particle confined in the "potential" given by $U_{\mu}(R)+W_{\mu\mu}(R)$. But as we shall see in the following, the price we pay is that the channel potential is generally complicated and its analytical expression is difficult to obtain, so that additional approximations must be introduced. In Sec. III, we will use the Ritz variational principle to obtain the approximate ground channel potential $U_{\mu}(R)$ and the diagonal-coupling term $W_{\mu\mu}(R)$.

The introduction of hyperspherical coordinates enables one to separate out the radial correlation represented by α_{ij} from the Schrödinger equation. Similarly, the use of the Euler angles and $\hat{\mathbf{r}}_{ij}\cdot\hat{\mathbf{r}}_{ij,k}$ to specify the directions of $\hat{\mathbf{r}}_{ij}$ and $\hat{\mathbf{r}}_{ij,k}$ makes it possible to single out the angular correlation represented by $\hat{\mathbf{r}}_{ij}\cdot\hat{\mathbf{r}}_{ij,k}$. This technique has been proved to be suitable especially to the S wave for which the Schrödinger equation does not depend on the Euler angles. In the calculation carried out in this paper, Euler angles and $\hat{\mathbf{r}}_{ij}\cdot\hat{\mathbf{r}}_{ij,k}$ (instead of $\hat{\mathbf{r}}_{ij}$ and $\hat{\mathbf{r}}_{ij,k}$) are used. The detailed discussion of the Euler angles can be found in Ref. 14. Here, we only give the transformation Jacobian and the volume element in terms of the Euler angles,

$$J=-\frac{\sin\Theta\sin2\theta_{12}}{\sin\Theta_1\sin\theta_2}\ , \tag{31}$$

$$d\hat{\mathbf{r}}_{ij}d\hat{\mathbf{r}}_{ij,k}=\sin\theta_{12}d\theta_{12}[(\sin\Theta)d\Theta\,d\Phi\,d\Psi]\ . \tag{32}$$

III. CHANNEL POTENTIAL $U_{\mu}(R)$ AND THE DIAGONAL-COUPLING TERM $W_{\mu\mu}(R)$

A. Analytical expressions

In this paper we use the trial function given in Ref. 7, namely,

$$\Phi_{\mu}(R,\Omega)=N\sum_{i,j}f_{ij}\ , \tag{33}$$

with

$$f_{ij}=P_{ij}(\mathbf{r}_{ij})\frac{\sinh t(\pi/2-\alpha_{ij})}{\sin\alpha_{ij}\cos\alpha_{ij}}\ , \tag{34}$$

where the sum goes over the three possible combinations 12,31, and 23 to make $\Phi_{\mu}(R,\Omega)$ symmetric, N is the normalization constant, and t is the variational parameter. P_{ij} satisfies the two-body Schrödinger equation with zero energy and zero angular momentum,

$$\left[-\frac{1}{2m_{ij}}\frac{d^2}{dr_{ij}^2}V_{ij}\right]P_{ij}(r_{ij})=0\ . \tag{35}$$

The normalization constant is

$$N^{-2}=3\langle f_{12}\,|\,f_{12}\rangle+6\langle f_{12}\,|\,f_{13}\rangle\ , \tag{36}$$

$$\langle\Phi_{\mu}\,|\,U(R)\,|\,\Phi_{\mu}\rangle=3N\langle\Phi_{\mu}\,|\,U(R)\,|\,f_{13}\rangle\ , \tag{37}$$

and

$$\langle\Phi_\mu|U(R)|f_{12}\rangle=-\frac{4+t^2}{2mR^2}\langle\Phi_\mu|f_{12}\rangle+\frac{t}{mR}\left\langle\Phi_\mu\left|\frac{P'_{12}\cosh t(\pi/2-\alpha_{12})}{\sin\alpha_{12}}\right\rangle\right.$$
$$+\langle\Phi_\mu|(V_{23}+V_{13})|f_{12}\rangle+\langle\Phi_\mu|\sin^2\alpha_{12}V_{12}|f_{12}\rangle+\frac{1}{2mR}\left\langle\Phi_\mu\left|\frac{P'_{12}\sinh t(\pi/2-\alpha_{12})}{\cos\alpha_{12}}\right\rangle\right. . \quad (38)$$

In order to facilitate the calculation, some discussion of the properties of the potential $V(R,\Omega)$ is desirable. Firstly, as pointed out before, we have assumed two-body interaction between the particles, which means that generally we can write $V(R,\Omega)$ as

$$V(R,\Omega)=V_{12}+V_{13}+V_{23} , \quad (39)$$

with

$$V_{ij}=V_{ij}(\mathbf{r}_{ij}) . \quad (40)$$

As for the two-body potential $V_{ij}(\mathbf{r}_{ij})$, we require that it is a short-range potential with a normal range b (note, the terminology "normal range" is used here in order to distinguish b from the effective range r_0).

Except for the above restrictions, the potential is arbitrary. Equations (36), (37), and (38) apply quite generally; however, $U_\mu(R)$ depends upon the detailed shape of the two-body potential V_{ij}. We are interested in the situation where $c_{ij}\gg b$. In this case we can neglect terms of order b/c_{ij} compared with unity. The $U_\mu(R)$ does not depend upon the details of the potential; rather, it depends only upon c_{ij}.

Based on the discussion above, Eq. (35) can be solved exactly outside the range of the potential; we get

$$P_{ij}=1-\frac{r_{ij}}{c_{ij}} , \quad (41)$$

where c_{ij} is the scattering length for the system of the particles i and j. But since identical particles are being considered here, we still have

$$c_{ij}=c_{jk}=c_{ik}\equiv c_0 . \quad (42)$$

Now, with the help of Euler angles, the normalization constant and the potential matrix element can be calculated straightforwardly. We obtain

$$N^{-2}\cong A_0+A_1R+A_2R^2 , \quad (43)$$

with

$$A_0=\frac{3}{2t}(\sin\pi t-\pi t)+\frac{4\pi}{\sqrt{3}t}\left[\sinh\frac{2\pi t}{3}-2\sinh\frac{\pi t}{3}\right] , \quad (44)$$

$$A_1=-\frac{6}{c_0}\left[\frac{\cosh\pi t}{1+4t^2}-1\right]+\frac{48}{\sqrt{3}c_0}\frac{1}{1+4t^2}\left[3t\sinh\frac{\pi t}{3}-t\sinh\frac{2\pi t}{3}+\frac{\sqrt{3}}{2}\left[\cosh\frac{\pi t}{3}-\cosh\frac{2\pi t}{3}\right]\right] , \quad (45)$$

$$A_2=\frac{3}{4c_0^2}\left[\frac{\sin\pi t}{t(1+t^2)}-\pi\right]+\frac{6}{\sqrt{3}c_0^2}\left[\frac{\sqrt{3}}{2t}\left[\sinh\frac{2\pi t}{3}-\sinh\frac{\pi t}{3}\right]-\frac{t}{2(1+t^2)}\left[\frac{2\pi}{3}\sinh\frac{\pi t}{3}+\frac{\pi}{3}\sinh\frac{2\pi t}{3}\right]\right.$$
$$\left.+\frac{\sqrt{3}}{2(1+t^2)}\left[\frac{\pi}{3}\cosh\frac{2\pi t}{3}-\frac{2\pi}{3}\cosh\frac{\pi t}{3}\right]\right] , \quad (46)$$

and

$$\langle\Phi_\mu|U|\Phi_\mu\rangle\simeq-\frac{4+t^2}{2mR^2}+\frac{3N^2}{mR^2}\sinh\frac{\pi t}{2}\left[t\cosh\frac{\pi t}{2}-\frac{8}{\sqrt{3}}\sinh\frac{\pi t}{6}\left[1-\frac{\sqrt{3}R}{2c_0}\right]\right]$$
$$+\frac{3N^2}{2mRc_0}\left[1-\cosh\pi t-\frac{\pi R}{4c_0}+\frac{R(1+2t^2)}{4c_0t(1+t^2)}\sinh\pi t+4\left[\cosh\frac{\pi t}{3}-\cosh\frac{2\pi t}{3}\right]\right.$$
$$+\frac{R}{c_0t}\left[\sinh\frac{2\pi t}{3}-\sinh\frac{\pi t}{3}\right]+\frac{R(1+2t^2)}{C_0(1+t^2)}\left[\frac{\pi}{3}\cosh\frac{2\pi t}{3}-\frac{2\pi}{3}\cosh\frac{\pi t}{3}\right]$$
$$\left.+\frac{Rt}{\sqrt{3}c_0(1+t^2)}\left[\frac{\pi}{3}\sinh\frac{2\pi t}{3}+\frac{2\pi}{3}\sinh\frac{\pi t}{3}\right]\right] . \quad (47)$$

In Eqs. (43)–(47), terms proportional to $b\eta/R^2$, where η is of the order unity, have been neglected. This is consistent with our conditions that $b \ll R$ and $b \ll c_0$.

B. Asymptotic behavior

(a) When the scattering length c_0 goes to infinity, we get, from Eqs. (43)–(47),

$$N^{-2}=\frac{3}{2t}(\sin\pi t-\pi t)+\frac{4\pi}{3t}\left[\sinh\frac{2\pi t}{3}-2\sinh\frac{\pi t}{3}\right], \tag{48}$$

$$\langle\Phi_\mu\mid U\mid\Phi_\mu\rangle=-\frac{4+t^2}{2mR^2}+\frac{3N^2}{mR^2}\sinh\frac{\pi t}{2}\times\left[t\cosh\frac{\pi t}{2}-\frac{8}{\sqrt{3}}\sinh\frac{\pi t}{6}\right], \tag{49}$$

in agreement with Ref. 7. In that case,

$$t\cosh\frac{\pi t}{2}-\tfrac{8}{3}\sinh\frac{\pi t}{6}=0 \tag{50}$$

determines the value of t which gives the relative minimum of the potential curve. Although Eq. (50) possesses an infinite number of complex roots, it has only one real root $t=1.006$. Hence the relative potential curve is given by Eq. (2). Notice that in this case, the hyperradial potential exhibits an effective term $1/R^2$ even at large distance R, which certainly supports an infinite number of bound states of the system.

(b) When c_0 is finite, from the expression of the trial function, we expect that the results in (a) can be reproduced as R goes to zero. It is not difficult to see that this is just the case. In fact, as $R\to 0$, Eqs. (43)–(47) reduce to Eqs. (48) and (49).

(c) When c_0 is finite and R is large, we expect that

$$\Phi_\mu=\text{const}\ .$$

which is proportional to the lowest-order hyperspherical harmonic and hence is the exact solution to the angular equation. We recover this function by letting $t=i$.

In Eqs. (43)–(47), letting $t=i$ and, at the same time, changing the signs of N^2 and the potential, we get

$$N^{-2}=A'_0+A'_1R+A'_2R^2\ , \tag{51}$$

$$U_\mu(R)=-\frac{3}{2mR^2}-N^2\left[\frac{4\sqrt{3}}{m}\frac{1}{R^2}+\frac{3}{mc_0}\frac{1}{R}-\frac{27\pi}{16mc_0^2}\right], \tag{52}$$

with

$$A'_0=\frac{7\pi}{2}\ , \tag{53}$$

$$A'_1=-\frac{12}{c_0}\ , \tag{54}$$

$$A'_2=\frac{9\pi}{8c_0^2}\ . \tag{55}$$

Hence, with c_0 finite, when R goes to infinity, we have

$$U_\mu(R)=\frac{C_1}{R^3}+\frac{C_2}{R^4}\ , \tag{56}$$

with

$$C_1=\frac{40c_0}{3m\pi}\ ,$$

$$C_2=\frac{C_0}{m}\left[20\left(\frac{8}{3\pi}\right)^2-\frac{32\sqrt{3}}{9\pi}-\frac{14}{3}\right]>0\ .$$

In this case, we do not have the inverse-square-potential term $1/R^2$. Of course, this is consistent with Efimov's result, since if we still had the $1/R^2$ potential term, the infinite number of bound states would also appear, which, in turn, is not what we expected for the case of finite scattering length.

Note that when $c_0>0$, the $1/R^3$ term is repulsive, in contradiction to what one obtains if we used $\Phi_\mu=\text{const}$ everywhere. This just illustrates the inadequacies of the zero-energy solution of Eq. (35) for $P_{ij}(\mathbf{r}_{ij})$ when $c_0>0$. Recall that when $c_0>0$, there is a low-energy two-particle bound state with

$$P_{ij}(r_{ij})\sim e^{-r_{ij}/c_{ij}}\ .$$

The effective-range expression, Eq. (41), just represents an expansion of the exponential in which the first two terms are kept. A more appropriate trial function would be the exponential. We do not consider this more elaborate trial function here since it only affects the region $R\gg c_{ij}$ which is unimportant for binding.

C. Numerical analysis

According to the Ritz variational principle, we vary the parameter t to get a relative minimum of the potential curve. The potential curve thus obtained gives an upper bound to the real one. Since R and c_{ij} appear in the trial function as a combination of R/c_{ij}, we discuss in detail only the potential curve for $c_0=30$ here. As for the potential curve with other positive scattering lengths, we give only the final results. Their detailed qualitative results can be obtained from those of $c_0=30$ by just changing the scale of hyper-radius R. The potential curves with negative scattering lengths have characteristics similar to those of the potential curves with positive scattering lengths.

Numerical results show that as R goes to 0, $t_{\min}$, which gives a minimum upper bound of the potential curve, goes to 1.006. This is what we expected, since as far as the asymptotic behavior of the potential curve is concerned, $R\to 0$ is equivalent to letting $c_0\to\infty$.

But, on the other hand, as R goes to infinity, $t_{\min}\to 0$. This is not what we want, since for $t=0$, the trial function (34) reduced to

$$f_{ij} \sim \frac{\pi/2-\alpha_{ij}}{\cos\alpha_{ij}} ,$$

which is not a good representation of the wave function at large R. In fact, since we let t vary as a real number in the computation, $t_{\min}=i$ cannot be obtained by this process. We found that if R is large enough, the potential curve with $t=i$ indeed goes below the potential curve with t equal to $t_{\min}$. Since the derivative of the potential need not be continuous (in fact, as a mathematical model, even the potential itself is allowed to be discontinuous at a finite number of points), the fact just mentioned suggests that when $R<R_t$, we take $U_\mu(t=t_{\min})$ and when $R>R_t$, we choose $U_\mu(t=i)$, where R_t is the largest hyper-radius at which the two potential curves cross. Moreover, for positive scattering length, in order to keep self-consistency as discussed in Sec. III B, it is better to set $U_\mu=0$ for R such that $U_\mu(R)$ calculated with Eq. (56) becomes positive. We should point out again here that this mandatory condition for positive scattering length affects only the long-range part of the potential curve and hence does not affect the analysis of the bound states in the energy region considered in this paper.

Figure 2 shows three potential curves with different scattering lengths. The values of the scattering lengths given there are chosen arbitrarily. We have also computed the potential curve for $c_0=-1000$, and the result appearing on Fig. 2 coincides with the potential curve with $c_0=500$ (see also Table I). It is not surprising that, except for the potential curve with $c_0=30$, the other three curves almost coincide, since for large scattering length, the second term in Eq. (41) can be neglected and the effective potential does not depend strongly on c_0. Also, Table I compares these potential curves with Eq. (2), the potential curve with infinite scattering length. The general results are exactly the same as analyzed in Sec. III B. Notice particularly the approximate coincidence of the potential curve with $c_0=-1000$ with Eq. (2) for R smaller than 50. Also notice particularly the deviation of the potential curve with $c_0=30$ from Eq. (2) for R larger than 5.

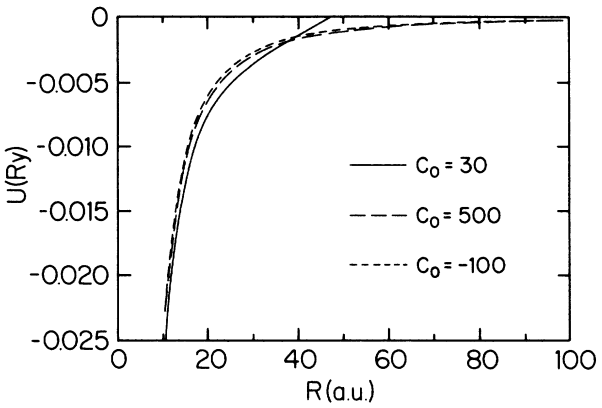

FIG. 2. Comparison of the potential curves with different scattering lengths, where Ry is the Rydberg unit.

D. Diagonal-coupling term $W_{\mu\mu}$

Since the channel function $\Phi_\mu(R,\Omega)$ is normalized, it is easy to show that the matrix element of the first derivative with respect to R between $\Phi_\mu(R,\Omega)$ vanishes. Hence from Eq. (29) the diagonal-coupling term is simply given by

$$W_{\mu\mu}=-\frac{1}{2m}\left\langle \Phi_\mu \left| \frac{d^2}{dR^2} \right| \Phi_\mu \right\rangle . \tag{57}$$

Now, if we write

$$\Phi_\mu = N\Phi_\mu$$

and take directly the second derivative of Φ_μ with respect to R, using once again the normalization property of Φ_μ, we get

$$\left\langle \Phi_\mu \left| \frac{d^2}{dR^2} \right| \Phi_\mu \right\rangle = \tfrac{1}{4}N^4 \left[\frac{dN^{-2}}{dR} \right]^2 - \tfrac{1}{2}N^2 \frac{d^2N^{-2}}{dR^2} , \tag{58}$$

where N^{-2} is given in Eq. (43).

For large R where t does not depend on R, we simply

TABLE I. Comparison of the potential curves with finite scattering length with Eq. (2).

R \ c_0	30	500	$U_\mu(R)$ -100	-1000	Eq. (2)
0.25	−40.190 77	−40.105 55	−40.072 97	−40.097 40	−40.100 12
0.50	−10.070 48	−10.027 75	−10.011 46	−10.023 67	−10.025 03
1.00	−2.252 07	−2.507 62	−2.499 48	−2.505 58	−2.506 26
2.00	−0.638 06	−0.627 24	−0.623 18	−0.626 22	−0.626 56
5.00	−0.104 95	−0.100 52	−0.098 91	−0.100 11	−0.100 25
10.00	−0.027 51	−0.025 20	−0.024 40	−0.024 99	−0.025 06
20.00	−0.007 57	−0.006 33	−0.005 94	−0.006 23	−0.006 27
30.00	−0.003 45	−0.002 83	−0.002 57	−0.002 76	−0.002 78
40.00	−0.001 35	−0.001 60	−0.001 41	−0.001 55	−0.001 57
50.00	−0.000 00	−0.001 03	−0.000 88	−0.000 99	−0.001 00
100.00	−0.000 00	−0.000 26	−0.000 20	−0.000 24	−0.000 25

have

$$\left\langle \Phi_\mu \left| \frac{d^2}{dR^2} \right| \Phi_\mu \right\rangle = \frac{1}{4} \frac{(A_1+2A_2R)^2}{(A_0+A_1R+A_2R^2)^2} - \frac{A_1}{A_0+A_1R+A_2R^2} . \quad (59)$$

It is important to notice that, similar to the channel potential curve, the $1/R^2$ term in Eq. (59) vanishes when R goes to infinity. Also, for infinite scattering length, the diagonal-coupling term become zero. On the other hand, the numerical result for $W_{\mu\mu}$ shows that when R is small, the diagonal-coupling term is much less than $U_\mu(R)$. However, as R becomes large, $W_{\mu\mu}$ has the magnitude of nearly one tenth of $U_\mu(R)$, so that generally it cannot be neglected for loosely bound states.

IV. POSSIBLE LOOSELY BOUND STATES OF THE SYSTEM

Having obtained the potential curve and the diagonal-coupling term, the radial equation (27), which is simply an effective one-dimensional Schrödinger equation, can now be solved directly. To see this, let

$$F_\mu(R)=R^{-5/2}Y(R) , \quad (60)$$

and then Eq. (27) becomes

$$\left[-\frac{1}{2m} \left[\frac{d^2}{dR^2} - \frac{\frac{15}{4}}{R^3} \right] + U_\mu + W_{\mu\mu} \right] Y = EY , \quad (61)$$

where $\frac{15}{4}/R^2$ behaves just as the angular barrier. Hence the effective potential is given by

$$V_{\text{eff}}(R)=\frac{1}{2m}\frac{\frac{15}{4}}{R^2}+U_\mu+W_{\mu\mu} . \quad (62)$$

From the expression of $U_\mu(R)$ and $W_{\mu\mu}(R)$, we can see that $2mV_{\text{eff}}(R)$ does not depend on m. m enters Eq. (61) only in combination with the bound-state energy E. Hence, in the numerical solution to Eq. (61), the choice of m affects only the units of E. In the following, we still simply set $m=1$.

The approximate wave function at large R can be obtained by the WKB method. Namely,

$$Y=\frac{1}{K(R)}\exp\left[-\int_R K(R)dR\right] , \quad (63)$$

where

$$K(R)=2mV_{\text{eff}}(R)-2mE . \quad (64)$$

The wave function given by Eq. (63) describes approximately the radial behavior of the system for $R>R_\infty$, where R_∞ is chosen so that for $R>R_\infty$, we have

$$K^2(R) \gg |K'(R)| , \quad (65)$$

which is the condition for the WKB method to be applicable. Hence R_∞ should be large enough so that $|E| \gg V_{\text{eff}}(R)$ or the effective potential varies with R very smoothly. Another reason to choose R_∞ large is that for the loosely bound states we are dealing with, the potential curve at large R has a significant effect on the radial wave function $F_\mu(R)$. Once the condition (65) is satisfied, the relative error of using Eq. (63) as the approximate wave function for $R>R_\infty$ should not be greater than

$$\left| \frac{K'(R)}{K^2(R)} \right|^2 .$$

The first derivative of Y with respect to R when $R>R_\infty$ is approximately given by

$$Y'=-\left[K(R)+\frac{K'(R)}{2K(R)}\right]Y . \quad (66)$$

After R_∞ is determined, we start with the boundary values of Y and Y' at R_∞, integrate Eq. (61) inward, and then we compute the ratio

$$B(E)=\left.\frac{Y'(R)}{Y(R)}\right|_{R_0} \quad (67)$$

at $R_0=2$, 4, and 6, respectively. The results are given in Figs. 3–5.

In order to obtain the energy of the possible loosely bound states, we need to know the logarithmic derivative on the boundary $R=R_0$ of a solution to the fully many-particle Schrödinger equation which satisfies appropriate

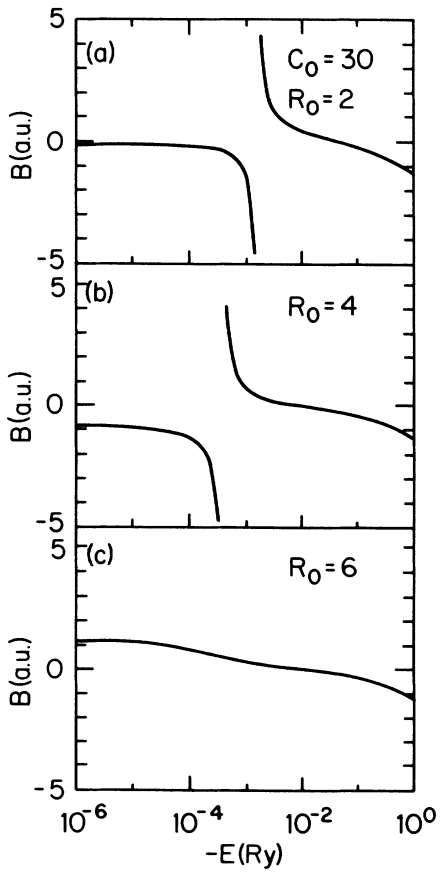

FIG. 3. Logarithmic derivation $B(E)$ on the boundary $R_0=2$, 4, and 6 for $c_0=30$, where Ry is the Rydberg unit.

boundary conditions at $R=0$. We call this logarithmic derivative $B_{\text{in}}(E)$. A solution satisfying boundary conditions everywhere only occurs for specific eigenenergies determined by the eigenvalue equation

$$B_{\text{in}}(E)=B(E) . \tag{68}$$

We are not trying to find the exact solution for small R in this paper. However, although we do not know the exact potential curve in the region R smaller than R, we can expect that the interaction in this region is generally much stronger than that in the outside region. Namely, the effective potential energy will be much larger than the loosely bound state energy. Therefore the wave function in the inside region, and hence $B_{\text{in}}(E)$, should not depend strongly on the energy. Since $B_{\text{in}}(E)$ is only a slowly varying function of E, we might, as an approximation, consider $B_{\text{in}}(E)$ as being independent of E. Therefore $B_{\text{in}}(E)$ will appear on Figs. 3–5 only as a horizontal straight line. The crossing points of the curves of $B_{\text{in}}(E)$ and $B(E)$ will determine the number and binding energies of the possible bound states for the system. From this argument, we conclude that in the energy region considered here, Figs. 3–5 [except Figs. 3(c) and 5(c)] show that the system has one or two bound states [probably three as in Fig. 4(a)].

From the figures, we also notice that, for a given finite scattering length, the number of bound states decreases with the increase of R_0. For $R_0=6$, if the magnitude of the scattering length is not large enough, the bound states might disappear. This is not difficult to understand. Since the channel potential $U_\mu(R)$ is independent of R_0, increasing R_0 means taking away the more attractive part of the potential from the system. Recalling that the choice of R_0 affects the accuracy of the results and depends on the range b of the two-body potential, it seems that for a given finite scattering length, the shorter the range of the potential, probably the more bound states will exist in the system.

Some comparisons of our results with Efimov's are given in Table II. From Fig. 4(a), we can also roughly estimate the magnitude of the spacing between two bound states,

$$\frac{E_N}{E_{N+1}}\sim 250 .$$

This is comparable with Efimov's result for infinite scattering length,

$$\frac{E_N}{E_{N+1}}\sim 500 .$$

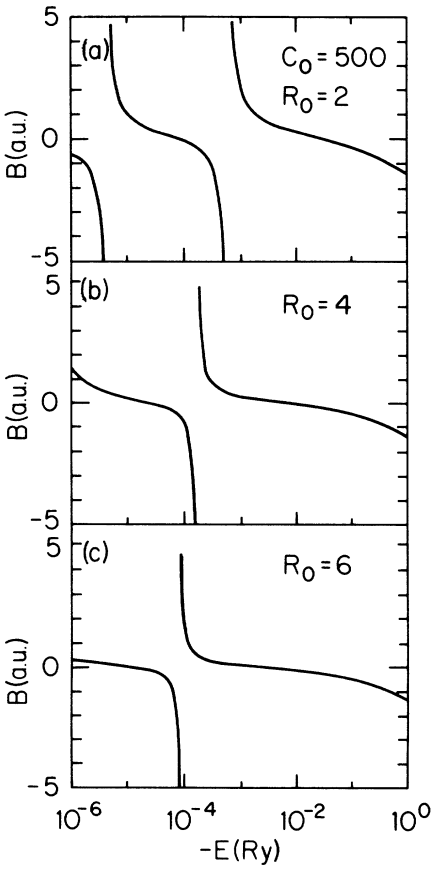

FIG. 4. Logarithmic derivative $B(E)$ on the boundary $R_0=2$, 4, and 6 for $c_0=500$, where Ry is the Rydberg unit.

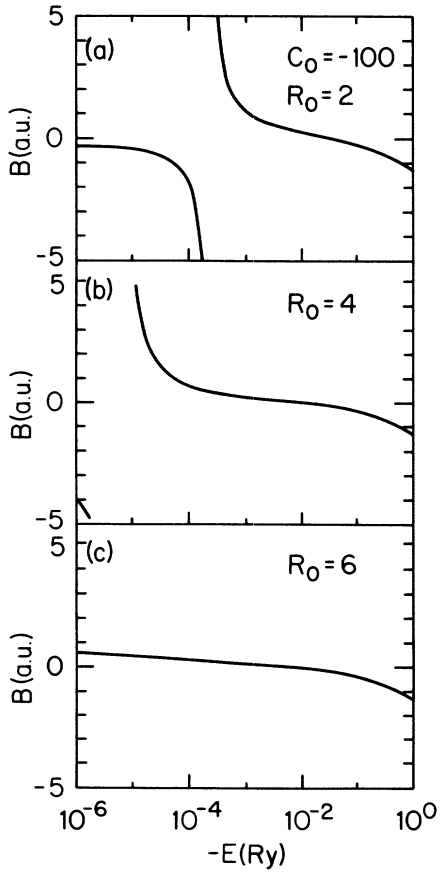

FIG. 5. Logarithmic derivative $B(E)$ on the boundary $R_0=2$, 4, and 6 for $c_0=-100$, where Ry is the Rydberg unit.

TABLE II. Number of loosely bound states.

	Number of bound states predicted by present work			Number of bond states[a] predicted by Efimov [Eq. (1)]		
c_0	$R_0=2$	$R_0=4$	$R_0=6$	$R_0=2$	$R_0=4$	$R_0=6$
30	1 or 2	1 or 2	0 or 1	0.86	0.64	0.51
500	2 or 3	1 or 2	1 or 2	1.75	1.54	1.41
−100	1 or 2	0 or 1	0 or 1	1.25	1.02	0.89
−1000	1 or 2	1 or 2	1 or 2	1.98	1.76	1.63

[a] r_0 is roughly chosen as R_0.

V. DISCUSSION

In this paper, using the adiabatic hyperspherical approach, we have shown quantitatively the prediction by Efimov given in Eq. (1). Although the result is still approximate in the sense that we neglect higher-order terms in b/R for the whole calculation, it nevertheless suggests a technique for solving exactly the ground channel eigenvalue problem of a three-body system. This, once again, demonstrates the adiabatic hyperspherical method as a comprehensive framework for quantitative treatment of three-body states.

Certainly the detection of the bound states predicted in this paper requires experimental techniques with extremely high resolution. However, the remarkable point here is that it reveals some new characteristic changes from a two-body problem to a many-body system. This is embodied in the two conclusions we obtained in this paper. Firstly, two-body potentials which cannot support two-body bound states may bind three bodies together loosely; secondly, potentials which can bind two-body systems may not support any three-body bound states.

As we mentioned above, the determination of the number and binding energies of the bound states requires the calculation of $B_{\rm in}(E)$. In fact, there are several ways to do this. The standard one, of course, is to solve directly the Schrödinger equation of the system for the wave function $Y_{\rm in}(R)$ at $R<R_0$ and then $B_{\rm in}(E)$ is given by

$$B_{\rm in}(E)=\left.\frac{Y'_{\rm in}(R)}{Y_{\rm in}(R)}\right|_{R_0}. \tag{69}$$

This procedure usually requires the explicit knowledge of the two-body potential and leads us to deal directly with the complicated short-range interactions between the particles. Sometimes even the traditional analytical R-matrix theory cannot give a good representation of $Y_{\rm in}$ because of the slow convergence of the expansion. Here we point out that variational calculation of the R matrix has been proposed by Fano and Lee in 1973.[15] Using this method, we can determine $B_{\rm in}(E)$ by the variational principle.

ACKNOWLEDGMENTS

Support for this research by the U.S. Department of Energy, Office of Basic Energy Sciences, Division of Chemical Sciences is gratefully acknowledged. One of us (Z.Z.) wishes to acknowledge support from the University of Nebraska–Lincoln, Maude Hammond Fling Foundation.

[1] L. D. Faddeev, Zh. Eksp. Teor. Fiz. **39**, 1459 (1961) [Sov. Phys.—JETP **12**, 1014 (1961)].

[2] Charles J. Joachain, *Quantum Collision Theory* (North-Holland, Amsterdam, 1978), pp. 512–575, and references therein.

[3] R. A. Minlos and L. D. Faddeev, Zh. Eksp. Teor. Fiz. **41**, 1850 (1961) [Sov. Phys.—JETP **14**, 1315 (1962)].

[4] G. V. Skorniakov and K. A. Ter-Martirosian, Zh. Eksp. Teor. Fiz. **31**, 775 (1956) [Sov. Phys.—JETP **4**, 648 (1957)].

[5] G. S. Danilov, Zh. Eksp. Teor. Fiz. **40**, 498 (1961) [Sov. Phys.—JETP **13**, 349 (1961)].

[6] C. C. H. Leung and S. C. Park, Phys. Rev. **187**, 1239 (1969).

[7] V. Efimov, Yad. Fiz. **10**, 107 (1969) [Sov. J. Nucl. Phys. **10**, 62 (1970)]; Phys. Lett. **33B**, 563 (1970); Yad. Fiz. **12**, 1080 (1970) [Sov. J. Nucl. Phys. **12**, 589 (1971)].

[8] H. A. Bethe, Phys. Rev. **76**, 38 (1949).

[9] R. D. Amado and J. V. Nobel, Phys. Lett. **35B**, 25 (1971); T. K. Lim, Sister Kathleen Duffy, and William C. Damert, Phys. Lett. **38**, 341 (1977); H. S. Huber and T. K. Lim, J. Chem. Phys. **68**, 1006 (1978); H. S. Huber, Phys. Rev. A **31**, 3981 (1985).

[10] J. Macek, Z. Phys. D **3**, 31 (1986).

[11] E. A. Soloviev and S. I. Vinitsky, J. Phys. B **18**, L557 (1985).

[12] J. Macek and K. A. Jerjian, Phys. Rev. A **33**, 233 (1986); T. F. Smith, Phys. Rev. **120**, 1058 (1960); J. M. Feagin, J. Phys. B **17**, 2433 (1984).

[13] P. M. Morse and H. Feshbach, *Methods of Theoretical Physics* (McGraw-Hill, New York, 1953), pp. 1725–1731; J. Macek, J. Phys. B **1**, 831 (1968); Z. Zhen and J. Macek, Phys. Rev. A **34**, 838 (1986).

[14] A. K. Bhatia and A. Temkin, Rev. Mod. Phys. **36**, 1050 (1964).

[15] U. Fano and C. M. Lee, Phys. Rev. Lett. **31**, 1573 (1973); J. Macek, Phys. Rev. A **30**, 1277 (1984).